Research Square

Preprints are preliminary reports that have not undergone peer review. They should not be considered conclusive, used to inform clinical practice, or referenced by the media as validated information.

Enhanced Visible Light Photocatalytic Degradation of Fe-Doped ZnO Nanoparticles For Organic Dyes

Senthilkumar M (sreeviveka@gmail.com)
Srinivasan College of Arts and Science https://orcid.org/0000-0002-6485-1002

C. Arunagiri
Periyar E.V.R. College

Original Research

Keywords: Visible light, Photocatalytic degradation, ZnO, Doping

Posted Date: February 10th, 2021

DOI: https://doi.org/10.21203/rs.3.rs-173224/v1

License: This work is licensed under a Creative Commons Attribution 4.0 International License.
Read Full License

Abstract

$Fe_xZn_{1-x}O$ (x = 0, 0.05, 0.075, 0.1 M) nanoparticles based photocatalysts were synthesized by a chemical precipitation method and characterized using X-ray diffraction (XRD), scanning electron microscopy (SEM) with energy dispersive X-ray emission (EDX) and UV–Vis spectroscopy. The photocatalytic efficiency of $Fe_xZn_{1-x}O$ catalysts was assessed under visible light irradiation using the degradation of methylene blue (MB) and methyl orange (MO) dye in aqueous solution. The present investigation shows that the effect of optimized parameters (pH, catalyst dosage and initial dye concentration) and doping concentrations plays significant role in photocatalytic activity. The detailed photocatalytic mechanism for the enhancement of photocatalytic activity has also been proposed.

Introduction

In recent years, lot of hazardous organic pollutants such as toxic dyes and organic residuals are released into the environment from various industries [1, 2]. The degradation and complete mineralization are difficult because complex structure of the organic dyes. Among these organic dyes, methylene blue (MB:$C_{16}H_{18}N_3SCl$) and methyl orange (MO: $C_{14}H_{14}N_3NaO_3S$) are highly harmful to the environment, then poses a threat to the health of humans and animals [3]. Industrial wastewater treatment and recycling are fundamental objectives to secure the worldwide biological system and improve the quality of the environment. Various techniques have been extensively utilized for the degradation of pollutants from contaminated water sources [4, 5]. Among them, photocatalysis have emerged to be promising way for controlling the current environmental pollution at the massive scale. Especially, photocatalysis using semiconducting nanoparticles has attracted a great deal of attention in photocatalytic reaction because of its unique physical and chemical properties [6-8].

Many researchers recently developed a photocatalysis using metal oxide semiconductor nanoparticles, including Bi_2O_3, TiO_2, ZnO, and WO_3. Among these oxides of transition metal, zinc oxide (ZnO) is found very sensible in photocatalytic method due to their wide-bandgap, non-toxicity and high photosensitivity [9-11]. ZnO is a wide-bandgap semiconductor with a direct energy bandgap of ($E_g \approx 3.37$ eV) is comparable to TiO_2 [12, 13]. ZnO nanoparticles are especially attractive for many interesting nanotechnology applications such as transparent conductive coatings [14], electrode materials for dye-sensitized solar cells (DSSCs) [15], gas sensors [16] and electro-photo luminescent materials [17]. However, previous studies proved that the ZnO is more efficient catalyst for waste water treatment. Unfortunately, ZnO can only absorb UV light [18] and photocatalytic efficiency was also restricted by the electron–hole recombination, low adsorption ability and restricted reusability. To overcome this problem numerous reports focused on doping ZnO with transition metal (Fe, Co, Mn) ions [19], non-metal (N, C, S) ions [20] and noble metals loading (Ag, Au, Pd) [21] have been carried out. Combination of two semiconductors with various bandgap incredibly enhance the photocatalytic activity [22–24]. Compared with other methods co-precipitation [25] has several advantages such as low-temperature preparation, easy to handle and low-cost.

A substantial number of studies reported that the doping ZnO with transition metal ions has been widely studied for visible light photocatalysts [26, 27]. It has been discovered that 2% Fe doped ZnO degraded methyl orange up to 80.8% in 210 mins of sun-light irradiation. The Fe doped ZnO degrades MB in 4 h in sun light [28]. Zhang *et al.* investigated that the utilization of Fe/ZnO nanowires is obviously superior to that of P25 against MO [29]. The synthesized Fe-doped ZnO nanoparticle via sol–gel technique and degraded 2-chlorophenol in aqueous solution under solar irradiation by Abbad *et al.* [30]. The optimized dopant centralization of 0.5 wt% Fe, the greatest photocatalytic action was accomplished owing to the fact of small crystallite size and low band gap with a low oxidation–reduction potential [30]. In the present work, we present a different noble Fe-doped ZnO photocatalysts with doping levels in the range 0–0.1 mol% via co-precipitation method. The synthesized photocatalysts were characterized by XRD, SEM-EDX, FTIR, IV and UV-Vis spectrophotometer. Also, we analyze the photocatalytic activity of Fe-doped ZnO nanoparticles using of MB and MO dye under visible light irradiation.

Experimental

2.1 Preparation

For synthesis of Fe doped ZnO ($Fe_xZn_{1-x}O$) various mol.% ($x \approx 0$, 0.05, 0.075 and 0.1) of nanoparticles were prepared by co-precipitation method. The chemicals such as zinc nitrate hexahydrate [$Zn(NO_3)_2.6H_2O$], ferric nitrate nonahydrate [$Fe(NO_3)_2.9H_2O$] and sodium hydroxide [NaOH] used in the present study were of analytical grade obtained from Alfa Aesar chemicals, India. Double distilled water was used through the experiments.

In a typical synthesis, 1 M solution of zinc nitrate was prepared by dissolving 10 g of $Zn(NO_3)_2{\cdot}6H_2O$ in 100 mL distilled water. 2 M sodium hydroxide solution was prepared by dissolving 8g of NaOH in 200 mL distilled water. Under continuous stirring at room-temperature NaOH solution was added by drop-wise addition until pH reached to about 11. The stirring of the solution was continued at 80°C for 2h. After completing the reaction, the solution was cooled to room temperature and finally white color precipitates were obtained. The dried participate was calcined at 450°C for 1h to form ZnO nanoparticle powder. To synthesis various concentration of Fe doped ZnO nanoparticles, such as Fe = 0.05, 0.075 and 0.1 mol.%, 0.68 to 3.4 g of $Fe(NO_3)_2.9H_2O$ was added into the reaction mixture.

2.2 Characterization Techniques

UV–Vis absorbance spectra measurements were performed with a SYSTRONICS: AU-2707 double beam spectrophotometer to detect absorption over the range 190–900 nm. XRD patterns were recorded using a mini desktop X'PERT PRO X-ray diffractometer operated with $CuK\alpha_1$ radiation of wavelength 1.5406 Å with scanning rate of 2º 2θ min^{-1} (from 2θ = 10 to 80 ºC). Surface morphology and size of the samples were obtained using scanning electron microscope JEOL JS-6390 instrument attached with an energy dispersive X-ray spectroscopy (EDX). Fourier transform-infrared (FTIR) spectra of prepared photocatalysts were recorded by using a JASCO FTIR-410 spectrophotometer wavenumber in the range 4000-400 cm^{-1}

with a resolution of 2 cm^{-1} delivered with computer software. The pH of the solution was noted by using ELICO (LI-10T model) digital pH meter. The current–voltage (I–V) characteristic curves were recorded using Keithley electrometer 2400 model.

2.3 Evaluation of photocatalytic degradation

The visible light photocatalytic activities of the $Fe_xZn_{1-x}O$, various mol% (x = 0, 0.05, 0.075 and 0.1%) nanoparticles under UV light (8 Watts Philips UV lamp) were evaluated by the degradation of MB and MO. The photocatalytic tests were done in a submersion type photoreactor made of wooden chamber. The catalyst powders like undoped ZnO and Fe (0.05, 0.075 and 0.1%) doped ZnO nanoparticles at various pH (2, 4 and 6). Each sample were taken 10 mg was dissolved in 20 ml of 100 µm aqueous solution of MB and MO dye. Before starting the irradiation process, the above prepared solution was stirred in the dark for 1 hour, to establish the adsorption/desorption equilibrium. All samples solution was transferred into the inside of photoreactor for UV exposure. Every 30 mins, 2 ml of dye solution collected from samples for photocatalytic degradation test. The dye solutions with the undoped ZnO and Fe doped ZnO nanoparticles were exposed to UV light from 0 to 180 mins at room temperature. By using a UV visible spectrophotometer at λ_{max} of 664 and 464 nm, the effective degradation of MB and MO was noticed. The degradation efficiency was calculated using the following formula (Eq. 1).

$$\eta\ (\%) = [1-Ct/Co] \times 100\% \qquad (1)$$

Where Co is the initial concentration of the dye solution and Ct is the concentration of dye solution at different time interval.

Results And Discussion

3.1 X-ray diffraction (XRD)

Fig. 1(a) shows the powder XRD characteristic patterns for $Fe_xZn_{1-x}O$ (x≈0, 0.05, 0.075, 0.1%) nanoparticles obtained by co-precipitation method. All the diffraction peaks could be indexed to hexagonal structure of crystalline ZnO, which further confirmed from the JCPDS No. 36-1451 (a = 0.325 nm and c = 0.5207 nm) [31]. Wurtzite phase of ZnO [32] were obtained for all samples, with the following diffraction peaks (100), (002), (101), (102), (110), (103), (200), (112) and (201). There are no characteristic peaks of Fe phases or its oxides were not detected in any of the samples. Fig. 1(b) shows the slightly shifted to higher angle (right) of peaks observed in the 30–38° interval with the increasing of Fe doping content, indicating overlapping of peaks. The magnification of the primary peaks at 31.7, 34.4 and 36.3° were slightly shifted to lower angle (left) occurs in the $Fe_{0.075}Zn_{0.925}O$ sample. The ionic radii of Fe^{3+} and Zn^{2+} are different (Fe^{3+} = 0.64 Å and Zn^{2+} = 0.74 Å). The result revealed that Fe ions substituting into the ZnO [33]. The average crystalline sizes of the $Fe_xZn_{1-x}O$ nanoparticles were estimated by applying the Debye–Scherrer equation (Eq. 2) to the half intensity width of the (100), (002) and (101) peaks [34].

$$D = k\lambda / \beta \cos\theta \qquad (2)$$

Where k is the shape of factor of the particles (k= 0.9), β is the full width half maximum of the peak (FWHM), θ and λ are the incident of diffraction angle and wavelength of the X-rays (1.5406 Å), respectively. The lattice constants calculated from XRD are presented in Table 1. The average crystalline sizes are decreases as 23, 21, 16 and 12 nm for ZnO, $Fe_{0.05}Zn_{0.95}O$, $Fe_{0.075}Zn_{0.925}O$ and $Fe_{0.1}Zn_{0.9}O$, respectively. This evolution can be due to the distortion creates in the crystal lattice by the incorporation of the Fe ions. When increasing Fe doping level, the FWHM decreases suggesting an increase of the average crystallite size. The same results were reported by Jayachitra *et al.* [35] in Fe doped ZnO nanoparticles, Srinivasan *et al.* [36] in Mn doped ZnO and Nahm *et al.* [37] in V_2O_5 doped ZnO ceramics.

Table 1. The lattice parameters of $Fe_xZn_{1-x}O$ nanoparticles annealed at 450 °C.

Fe Doping Concentration (mol.%)	hkl	2θ (degree)	a[Å]	c[Å]	Crystallite size (nm)
ZnO	(100)	31.77	3.24		23.53
	(002)	34.40		5.20	
	(101)	36.30			
$Fe_{0.05}Zn_{0.95}O$	(100)	31.81	3.25		21.66
	(002)	34.23		5.21	
	(101)	36.34			
$Fe_{0.075}Zn_{0.925}O$	(100)	31.71	3.25		16.23
	(002)	34.43		5.20	
	(101)	36.37			
$Fe_{0.1}Zn_{0.9}O$	(100)	31.81	3.24		12.03
	(002)	34.23		5.21	
	(101)	36.33			

3.2 SEM Analysis

The surface morphologies of $Fe_xZn_{1-x}O$ (x≈0, 0.05, 0.075 and 0.1 mol.%) nanoparticles are shown in Fig. 2(a-d). Fig. 2(a) shows the surface morphology of undoped ZnO nanoparticles. It has an irregular structure with crystalline size of ~42-68 nm and having a better crystalline quality. The doping of 0.05 mol.% of Fe, ZnO nanoparticles are turned into irregular pores like structure [Fig. 2(b)]. On further doping of Fe from 0.075 to 0.1 mol.% in the Fe doped ZnO lattice resulted in the mixture of needle and spherical

like structure [Fig. 2(c-d)]. From the outcomes, it should be noticed that the samples were agglomerated and consists of small irregular pores. The images clearly exposed that undoped ZnO was prepared well with nanometer size and the surface morphology changed with the extension of Fe concentration. Compared with undoped ZnO, 0.1 mol.% of Fe-doped ZnO showed more information on the surface. It can also be noticed that the size and morphology of $Fe_xZn_{1-x}O$ nanoparticles enhanced with the dopant concentration.

3.3 EDX Analysis

EDX analysis (Fig. 3a–d) was carried out to investigate the elemental composition of $Fe_xZn_{1-x}O$ (x≈0, 0.05, 0.075 and 0.1 mol.%) nanoparticles. Fig. 3(a) reports the spectrum of undoped ZnO, showing the characteristic peaks associated with O and Zn elements. The measured atomic percentage of these elements is 49.5 and 50.5 at. %, respectively. Fig. 3(b–d) shows the EDX analysis of Fe doped ZnO nanoparticles. The inset of EDX image $Fe_xZn_{1-x}O$ nanoparticles data were given in table format. The measured Fe concentration of 0.05, 0.075 and 0.1 mol.%, are about 2.71, 14.94 and 18.21 at. % respectively. The EDX results confirm the presence of Fe, Zn and O are clearly observed at their normal energy. The observed atomic percentage values almost match well with the samples.

3.4 UV-Vis spectral studies

UV-absorption spectra of $Fe_xZn_{1-x}O$ (x≈0, 0.05, 0.075 and 0.1 mol.%) nanoparticles shown in Fig. 4 (a-d). The absorption edge is shifted towards higher wavelength region which means that the band gap decreases. The red-shift is due to the increase of crystallite size and it was confirmed from the XRD results. The optical bandgap (Eg) of ZnO and Fe doped ZnO nanoparticles were calculated by using the formula $Eg = hc/\lambda$ [38-40]. The calculated optical band gap Eg values are 3.90, 3.89, 3.86 and 3.82 eV which corresponds to undoped ZnO and 0.05, 0.075 & 0.1% Fe doped ZnO nanoparticles for the increasing doping level. Hassan *et al.* revealed that the absorbance also depends upon some factors like crystalline size, oxygen deficiency, defects in grain structure, lattice strain, thickness etc [41]. The replacement of Fe^{3+} with Zn^{2+} causes the creation of oxygen vacancies and additional energy levels, which reduces the band gap with the dopants.

3.5 FTIR Analysis

The FTIR spectra of $Fe_xZn_{1-x}O$ (x≈0 and 0.1 mol.%) nanoparticles in the range 4000–400 cm^{-1} to determine the presence of various functional groups shown in the Fig. 5 (a, b). The broad band located around 3452–3446 cm^{-1} corresponds to O–H stretching vibration of adsorbed water molecules, while the band located around 1625 and 1591 is due to O–H bending vibration of the same atmospheric water [42]. The bands with lower intensity absorbed at around 2380 cm^{-1}, and attributed to symmetric and asymmetric C–H bonds, respectively, appears due to an environmental contamination. The strong absorption band at 428 cm^{-1} is due to Zn–O stretching mode for undoped ZnO nanoparticles; similarly, for 0.1 mol.% Fe doped ZnO samples this is pointed out from absorption peaks in the range of 449 cm^{-1},

respectively. The small stretch observed at 601 cm^{-1} only found in the 0.1% Fe-doped ZnO sample, is characteristic of a Fe–O stretch as reported by Liu *et al.* [43]. Therefore, it might be due to Fe ions substituted by Zn ions and incorporated into the crystal lattice of ZnO. New absorption peaks at 1120, 1122 and 800 cm^{-1} appear on both samples was ascribed to the sulphate group [43].

3.5 I-V Characteristics

The I-V characteristics studies of $Fe_xZn_{1-x}O$ (x≈0 and 0.1 mol.%) nanoparticles have been carried out using silver paste to make good electrical contact shown in the Fig. 6 (a, b). From these curves, DC electrical conductivity measurement of $Fe_xZn_{1-x}O$ (x≈0 and 0.1 mol.%) nanoparticles taken under varying temperatures of 30, 50, 70, 90, 110 and 130 °C (Increase of 20 °C). Thus, increases the conductivity of 0.1% Fe doped ZnO nanoparticles due to increase the mobility of charge carriers [44]. The remarkable increase in the conductivity by these samples may results in higher advantage for electro-optic device fabrication.

3.6 Photodegradation of MB and MO

3.6.1 Effect of pH

The adsorption of MB and MO dye molecules on undoped ZnO nanoparticles strongly depends on the pH of the solution are displayed in Fig. 7(a). The effect of pH on the photodegradation of MB and MO dye was studied by varying the pH of the solution from 2 to 6. The outcome shows that photodegradation is high at base medium and afterward decreases when the pH of the solution decreases. The degradation arrives at most extreme at pH = 6 and afterward decreases sensibly up to pH = 2. Henceforth, the pH = 6 was accepted as ideal pH and utilized for additional investigation.

3.6.2 Effect of catalyst concentration

The effect of catalyst concentration on the photodegradation of MB and MO dye was tested using ZnO catalyst concentrations from 5 to 15 mg/50 ml in 10 ppm MB and MO dye solution at pH=6 are displayed in Fig. 7(b). The variation in photodegradation can be explained by the availability of number of surface-active sites and the immersion of UV light towards the dye solution. The results are displayed in Fig. 6; the figure visibly shows that the photodegradation reaches maximum at 10 mg/50 ml and higher catalyst concentration more than 15 mg/50 ml results in the decrease in photodegradation. The reduced photodegradation at higher catalyst concentration (15 mg/50 ml) may be due to the aggregation of ZnO nanoparticles. The aggregation of nanoparticles leads to the increase in scattering effect and, thereby decreases the active sites [45]. Consequently, 10 mg/50 ml ZnO photocatalyst is expected as ideal catalyst load.

3.6.3 Effect of UV irradiation time of MB

Photocatalytic experiments were carried out with an initial MB concentration of 2.0 mM, catalyst concentration of 10 mg, pH = 6 and irradiation time upto 180 min. The photocatalytic activity of MB dye

solution (10 PPM) was also studied for reference. Fig. 8(a-d) shows the change in absorption spectra of MB exposed to UV light for various irradiation times (0, 30, 60, 90, 120 and 150 min) in the presence of $Fe_xZn_{1-x}O$ (x≈0, 0.05, 0.075, 0.1 mol.%) nanoparticles. The absorption maxima at 664 nm decreased gradually with extension of irradiation time.

The MB dye was degraded under UV light almost completely within 150 min. in the presence of $Fe_xZn_{1-x}O$ (x≈0, 0.05, 0.075, 0.1 mol.%) nanoparticles shown in Fig. 8(e). The results revealed that the Fe doped ZnO showed higher photocatalytic activity than that of undoped ZnO. Fe (0.075 mol.%) doped ZnO showed enhanced photocatalytic activity with a degradation efficiency of 68% for MB (pH = 6) dye at 150 min. Where, Fe (0.075%) doped ZnO nanoparticles takes short period of time to degrade the MB dye compared to other concentration of the Fe doped ZnO nanoparticles. The reduction of photocatalytic activity at higher concentration Fe (0.1%) doped ZnO may be due to the reduced path length of photons [45]. The obtained results are similar to the results reported by Suganthi *et al.* for the photodegradation of malachite green (MG) [46]. Another reason for increase in photocatalytic activity of Fe doped ZnO nanoparticles is due to the fact that dopant incorporated on to the surface of the ZnO can suppress the recombination of electron–hole pairs due to enhance their efficiency [47, 48].

3.6.4 Effect of UV irradiation time of MO

Photocatalytic experiments were carried out with an initial MO concentration of 3.0 mM, catalyst concentration of 10 mg, pH = 6 and irradiation time upto 180 min. The photocatalytic activity of MO dye solution (10 PPM) was also studied for reference. The variation in absorption spectra of MO showing to UV light for various irradiation times (0, 30, 60, 90, 120 and 150 min) in the presence of $Fe_xZn_{1-x}O$ (x≈0, 0.05, 0.075, 0.1 mol.%) nanoparticles. The absorption maxima at 454 nm decreased gradually with extension of irradiation time shown in Fig. 9(a-d).

MO dye was degraded under UV light almost completely within 150 min. in the presence of $Fe_xZn_{1-x}O$ (x≈0, 0.05, 0.075, 0.1 mol.%) nanoparticles shown in Fig. 9(e). The results revealed that the Fe doped ZnO showed higher photocatalytic activity than that of undoped ZnO. Fe (0.075%) doped ZnO showed enhanced photocatalytic activity with a degradation efficiency of 55% for MO (pH = 6) dye at 150 min [49].

In this process narrow semiconductor act as sensitizer to enhance the photodegradation of the organic dye and it can produce more photons to excite the electrons from the valence to the conduction band. When the photocatalyst was illuminated with higher energy photons, it allws the oxidation of the dye molecule [45]. We have proposed a mechanism for the enhanced photocatalytic activity of Fe doped ZnO nanoparticles. It can be described as follows:

$ZnO + h\gamma \quad ZnO\ (h^+_{VB} + e^-_{CB})$ (3)

$(h^+_{VB}) + dye \quad dye^+_{VB}$ oxidation of dye molecule (4)

When ZnO is irradiated by visible light, holes (h^{+}_{VB}) and electrons(e^{-}_{CB}) are generated in its valence band and conduction band respectively. The photogenerated electrons and holes combine with Fe^{3+} ions respectively.

$Fe^{3+} + O_2$ $Fe^{5+} + O_2°-$ (electron release) (5)

$Fe^{3+} + OH^{-}$ $Fe^{2+} + OH^{\circ}$ (hole release) (6)

OH° + dye (MB & MO) oxidation of dye molecule (7)

These super oxide anion ($O_2°-$) and hydroxyl radicals (OH°) are powerful oxidizing species and it will degrade of MB and MO dye molecule (Eq. 7) [49]. From these results we can conclude that the surface of Fe doped ZnO nanoparticles has played a primary role in degradation of organic dyes.

Conclusion

In this paper, $Fe_xZn_{1-x}O$ (x≈0, 0.05, 0.075, 0.1 mol.%) nanoparticles were synthesized by co-precipitation method. The average crystallite size of $Fe_xZn_{1-x}O$ nanoparticles was found to be decreases when the doping concentration of Fe increases, which is confirmed by the XRD analysis. Doping with Fe modified the morphology of ZnO nanoparticles obtained. The particle size of the synthesized nanoparticles was found to be ~42-68 nm. UV-Vis absorbance studies revealed that the band gap decreases as the Fe concentration increases in comparison with undoped ZnO. The maximum percentage of MB and MO photodegradation was achieved with synthesized Fe-doped ZnO nanoparticles with dosage concentration of 10 mg and irradiation time of 150 min at pH = 6. $Fe_{0.075}Zn_{0.925}O$ nanoparticles may be used as an efficient photocatalyst for the degradation of organic pollutants under visible light.

References

1. Nezamzadeh-Ejhieh, N. Moazzeni, J. Ind. Eng. Chem. 19 (2013) 1433.
2. Safari, M. Nikazar, M. Dadvar, J. Ind. Eng. Chem. 19 (2013) 1697.
3. Arques, A., Amat, A. M., Garcia-Ripoll, A. & Vicente, R. Detoxification and/or increase of the biodegradability of aqueous solutions of dimethoate by means of solar photocatalysis. J. Hazard. Mater. 146 (2007) 447.
4. Gupta, V. K., Pathania, D., Agarwal, S. & P. Singh, Adsorption photocatalytic degradation of methylene blue onto pectin–CuS nanocomposite under solar light. J. Hazard. Mater. 243(179) (2012).
5. Korbahti, B. K., Artut, K., Gecgel, C. & Ozer, A. Electrochemical decolorization of textile dyes and removal of metal ions from textile dye and metal ion binary mixtures. Chem. Eng. J. 173(677) (2011).
6. Joo, J. B. *et al.* Controllable Synthesis of Mesoporous TiO2 Hollow Shells: Toward an Efficient Photocatalyst. Adv. Funct. Mater. 23(4246) (2013).

7. Yu, T.-H., Cheng, W.-Y., Chao, K.-J. & Lu, S.-Y. ZnFe2O4 Decorated CdS Nanorods as a Highly Efficient, Visible Light Responsive, Photochemically Stable, Magnetically Recyclable Photocatalyst for Hydrogen Generation. Nanoscale 5(7356) (2013).
8. Lima, D. Fernandes, M. Silva, M. Baesso, A. Neto, G. de Morais, et al., Co-doped ZnO nanoparticles synthesized by an adapted sol–gel method: effects on the structural, optical, photocatalytic and antibacterial properties, J. Sol–Gel Sci.Technol.72(2014)301–309.
9. Cao, B. & Cai, W. From ZnO nanorods to nanoplates: chemical bath deposition growth and surface-related emissions. J. Phys. Chem. C 112(680) (2008).
10. Saravanan, R. et al. ZnO/Ag/Mn_2O_3 nanocomposite for visible light induced industrial textile effluent degradation, uric acid and ascorbic acid sensing and antimicrobial activity RSC Adv 5(34645) (2015).
11. Saravanan, R. et al. ZnO/Ag nanocomposite: An efficient catalyst for degradation studies of textile effluents under visible light Materials Science and Engineering C 33(2235) (2013).
12. -Y. Lee, S.-J. Park, J. Ind. Eng. Chem. 19 (2013) 1761.
13. Liu, C. Li, J. Yu, Q. Xiang, CrystEngComm 13 (2011) 2533.
14. Rajesh, B. Varalakshmi, C.S. Sunandana, Phys. B 407 (2012) 4537e4539.
15. Arshad, M.M. Ansari, A.S. Ahmed, P. Tripathi, S.S.Z. Ashraf, A.H. Naqvi, A. Azam, J. Lumin. 161 (2015) 275e280.
16. Chow, O. Lupan, G. Chai, H. Khallaf, L.K. Ono, B.R. Cuenya, I.M. Tiginyan, V.V. Ursaki, V. Sontea, A. Schulte, Sens. Actuators A 189 (2013) 399e408.
17. X. Liua, Y.C. Liua, D.Z. Shena, G.Z. Zhonga, X.W. Fana, X.G. Konga, R. Muc, D.O. Hendersonc, J. Cryst. Growth 240 (2002) 152e156.
18. Bak, J. Nowotny, M. Rekas, C. Sorrell, Int. J. Hydr. Energy 27, 991–1022 (2002)
19. Han, L. Ren, Z. Cui, C. Chen, H. Pan, J. Chen, Appl. Catal. B: Environ. 126 (2012) 298.
20. S. Shinde, C.H. Bhosale, K.Y. Rajundoped, J. Photochem. Photobiol. B 113 (2012) 70.
21. Min, K. Zhang, Y. Chen, Y. Zhang, W. Zhao, Sep. Purif. Technol. 92 (2012) 115.
22. Shifu, C. Lei, G. Shen, C. Gengyu, Materials Chemistry and Physics, 98 (2006)116–120.
23. Park, W. Choi, M.R. Hoffmann, Journal of Materials Chemistry,18 (2008) 2379–2385.
24. Peng, Y. Huang, Y. Li, Materials Science in Semiconductor Processing16 (2013)62–69.
25. Rahmati, A.B. Sirgani, M. Molaei, M. Karimipour, Cu-doped ZnO nanoparticles synthesized by simple co-precipitation route, Eur.Phys.J.Plus129 (2014)7.
26. Malathy, K. Vignesh, M. Rajarajan, A. Suganthi, Ceram. Int. 40 (2014) 101.
27. M. Rajbongshi, S.K. Samdarshi, Appl. Catal. B: Environ. 144 (2014) 435.
28. Dong, S., Xu, K., Liu, J. & Cui, H. Photocatalytic performance of ZnO: Fe array films under sunlight irradiation. Physica B 406(3609) (2011).

29. Zhang, Y., Ram, M. K., Stefanalkos, E. K. & Goswami, D. Y. Enhanced photocatalytic activity of iron doped zinc oxide nanowires for water decontamination, Surf. Coat. Technol. 217(119) (2013).
30. M. Ba-Abbad, A.A.H. Kadhum, A. Mohamad, M.S. Takriff, K. Sopian, Visible light photocatalytic activity of Fe3+-doped ZnO nanoparticle prepared via sol-gel technique, Chemosphere, 91 (2013) 1604-1611.
31. A. Ashkarran, A. Irajizad, S.M. Mahdavi, M.M. Ahadian, ZnO nanoparticles prepared by electrical arc discharge method in water, Mater.Chem.Phys.118 (2009)6–8.
32. Zhou, F. Zhao, Y. Wang, Y. Zhang, and L. Yang, Size-controlled synthesis of ZnO nanoparticles and their photoluminescence properties, J. Lumin. 122–123 (2007) 195–197.
33. Bai, T.Guo, Y.Zhao, SunJ, D.Li, A.Chen, et al.,Sensing performance and mechanism ofFe-dopedZnOmicroflowers,Sens.ActuatorsB:Chem.195 (2014)657–666.
34. Nasir, S. Bagwasi, Y. Jiao, F. Chen, B. Tian, J. Zhang, Chem. Eng. J. 236 (2014) 388.
35. Jeyachitra, V. Senthilnathan, T. S. Senthil 'Studies on electrical behavior of Fe doped ZnO nanoparticles prepared via co-precipitation approach for photo-catalytic application, J Mater Sci: Mater Electron, 2017.
36. Srinivasan, J. Kumar, Cryst. Growth 310, 1841 (2008)
37. W. Nahm, J. Mater. Sci. Mater. Electron. 24, 70 (2013)
38. Viswanatha, Y.A. Nayaka, C.C. Vidyasagar, T.G. Venkatesh, J. Chem. Pharm. Res. 4 (4) (2012) 1983e1989.
39. C. Vidyasagar, Y.A. Naik, T.G. Venkatesh, R. Viswanatha, Powder Technol. 214 (2011) 337e343.
40. G. Venkatesh, Y.A. Nayaka, R. Viswanatha, C.C. Vidyasagar, B.K. Chethana, Power Tech. 225 (2012) 232-238.
41. M. Hassan, W. Khan, A. Azam, A.H. Naqvi, J. Ind. Eng. Chem. 21 (2015) 283-291.
42. Amalia Mesaros, Cristina D. Ghitulica, Mihaela Popa, Raluca Mereu, Adriana Popa, Traian Petrisor Jr., Mihai Gabor, Adrian Ionut Cadis, Bogdan S. Vasile, Synthesis, structural and morphological characteristics, magnetic and optical properties of Co doped ZnO nanoparticles, Ceram. Int. 40 (2014) 2835–2846.
43. Liu, D. Meng, H. Pang, X. Wua, J. Xie, X. Yu, L. Chen, X. Liu, J. Magn. Magn. Mater. 324, 3356 (2012).
44. Abed, H. Bougharraf, K. Bouchouit, Z. Sofiani, B. Derkowska-Zielinska, M.S. Aida, B. Sahraoui, Superlattice Microstruct. 85,370 (2015)
45. V. Elangovan, V. Chandramohan, N. Sivakumar & T.S. Senthil, Synthesis and characterization of ZnO nanoparticles at different molarity concentrations for photocatalytic applications, Desalination and Water Treatment, (2015) 1–8.
46. Vignesh, M. Rajarajan, A. Suganthi, Visible light assisted photocatalytic performance of Ni and Th co-doped ZnO nanoparticles for the degradation of methylene blue dye, Journal of Industrial and Engineering Chemistry, 20 (2014) 3826–3833.
47. Bousslama, H. Elhouichet, M. Ferid, Optik 134, 88 (2017)

48. Yu, D. Meng, C.Li.U.K. Xu, J. Chen, C. Lu, Y. Wang, J. Mater. Sci. 25, 3920 (2014)
49. K. Kansal, M. Singh, D. Sud, Studies on photodegradation of two commercial dyes in aqueous phase using different photocatalysts, J. Hazard. Mater. 141 (2007) 581–590.

Figures

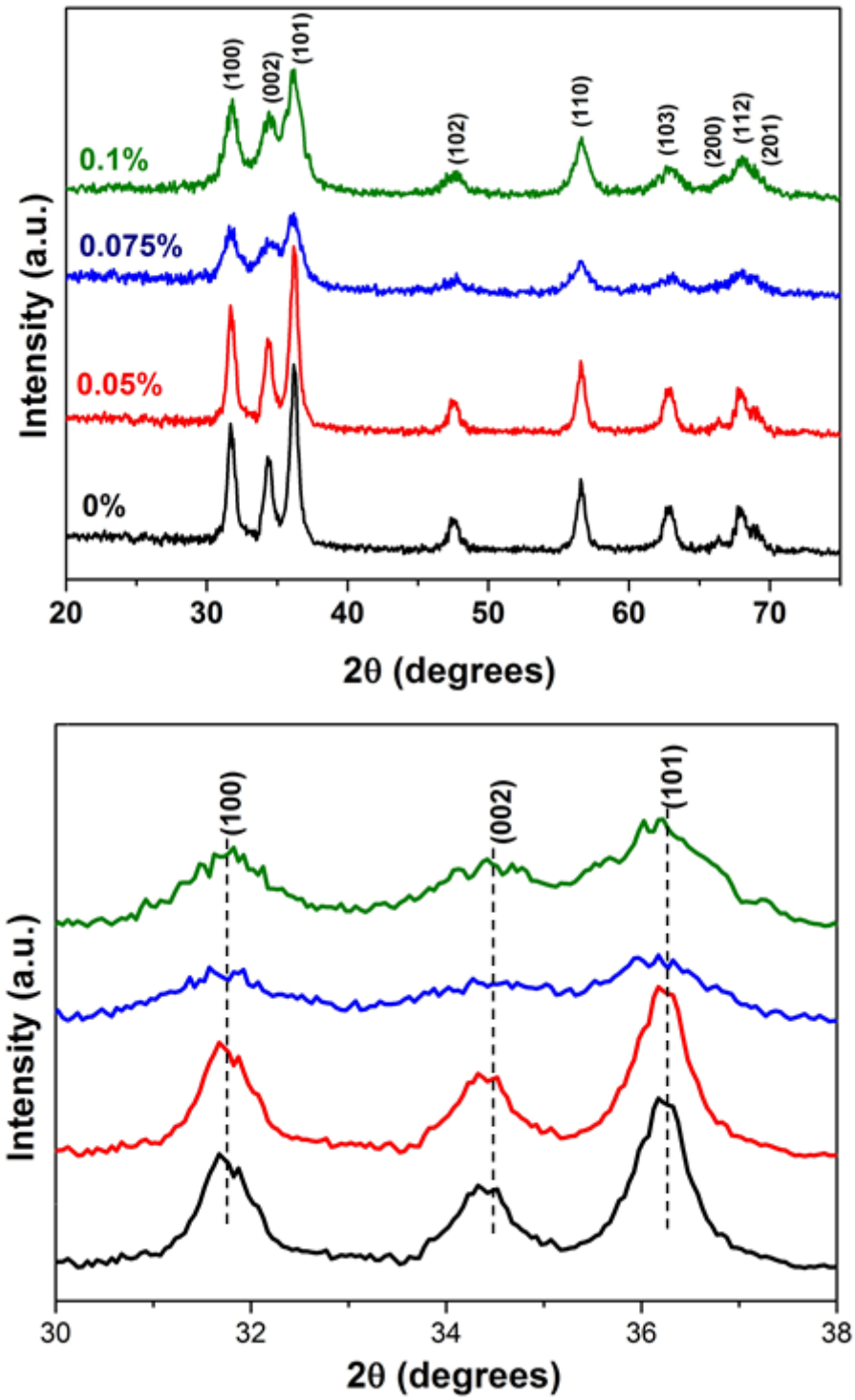

Figure 1

(a) XRD patterns of (a) undoped ZnO and Fe-doped ZnO (0.05, 0.075 & 0.1%) nanoparticles (b) Fe concentration dependent shift in primary diffraction peaks.

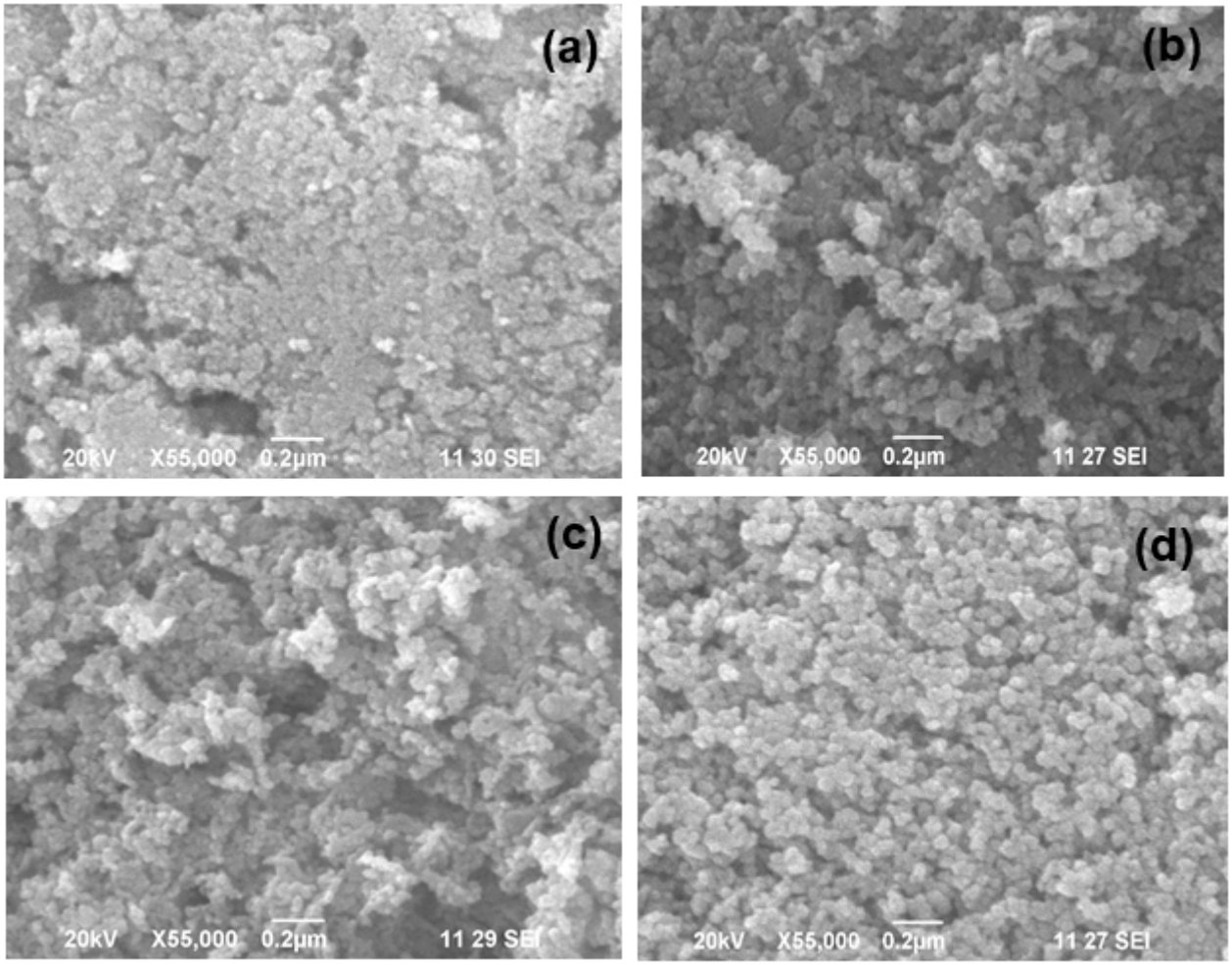

Figure 2

SEM images of FexZn1-xO nanoparticles with different molar ratio of (a) undoped ZnO (b) 0.05%, (c) 0.075% and (d) 0.1%

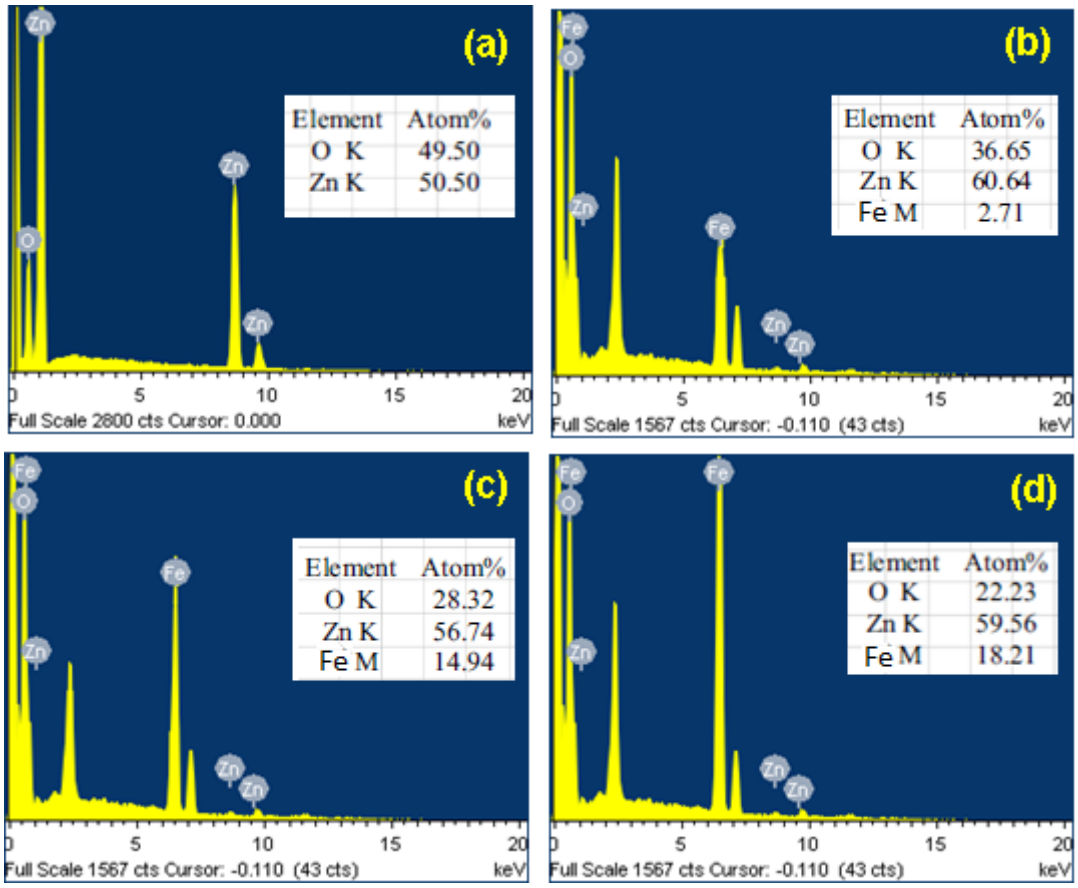

Figure 3

EDX images of FexZn1-xO nanoparticles: (a) undoped ZnO (b) 0.05%, (c) 0.075% and (d) 0.1%

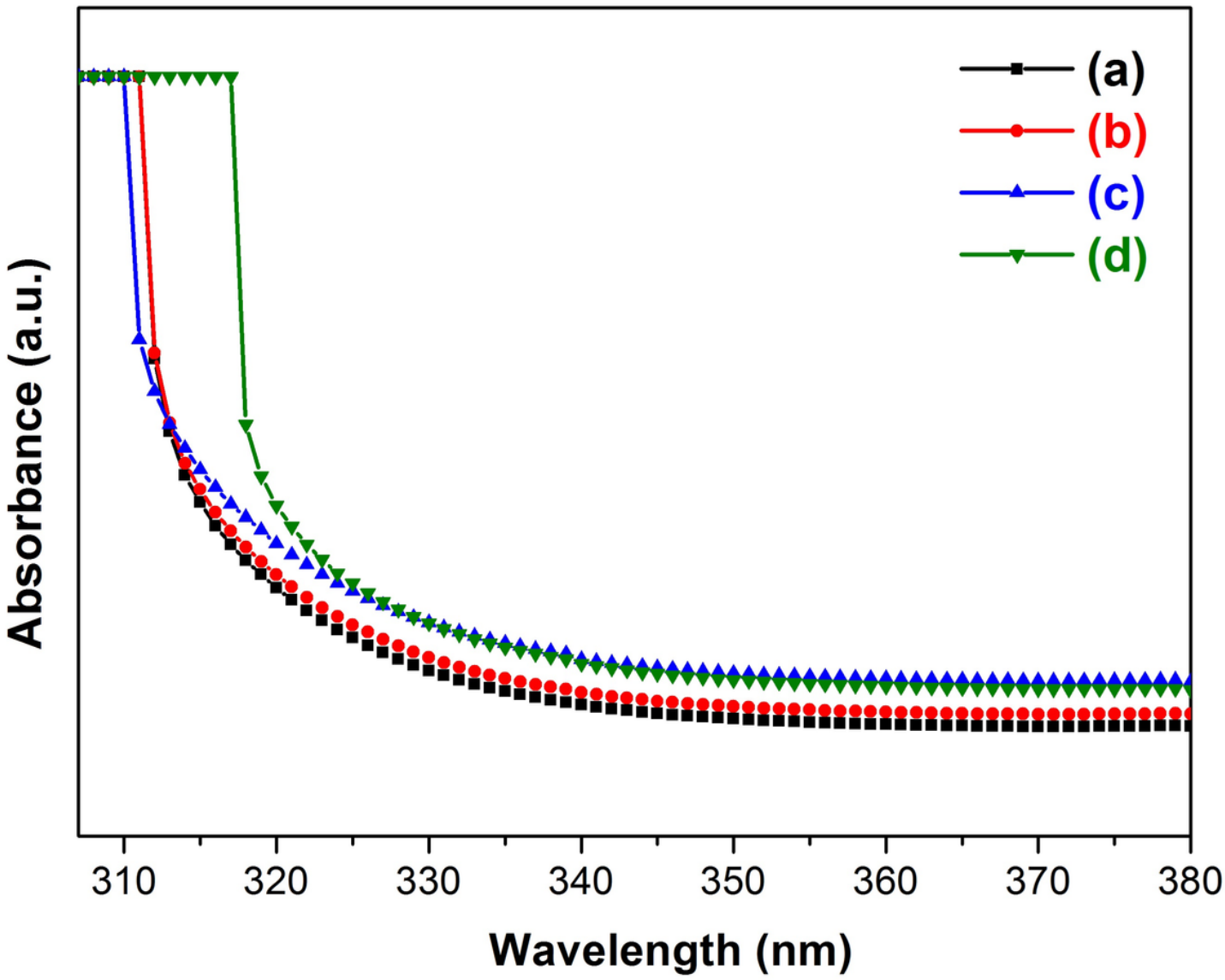

Figure 4

UV-Vis absorbance spectra of FexZn1-xO nanoparticles: (a) undoped ZnO (b) 0.05%, (c) 0.075% and (d) 0.1%

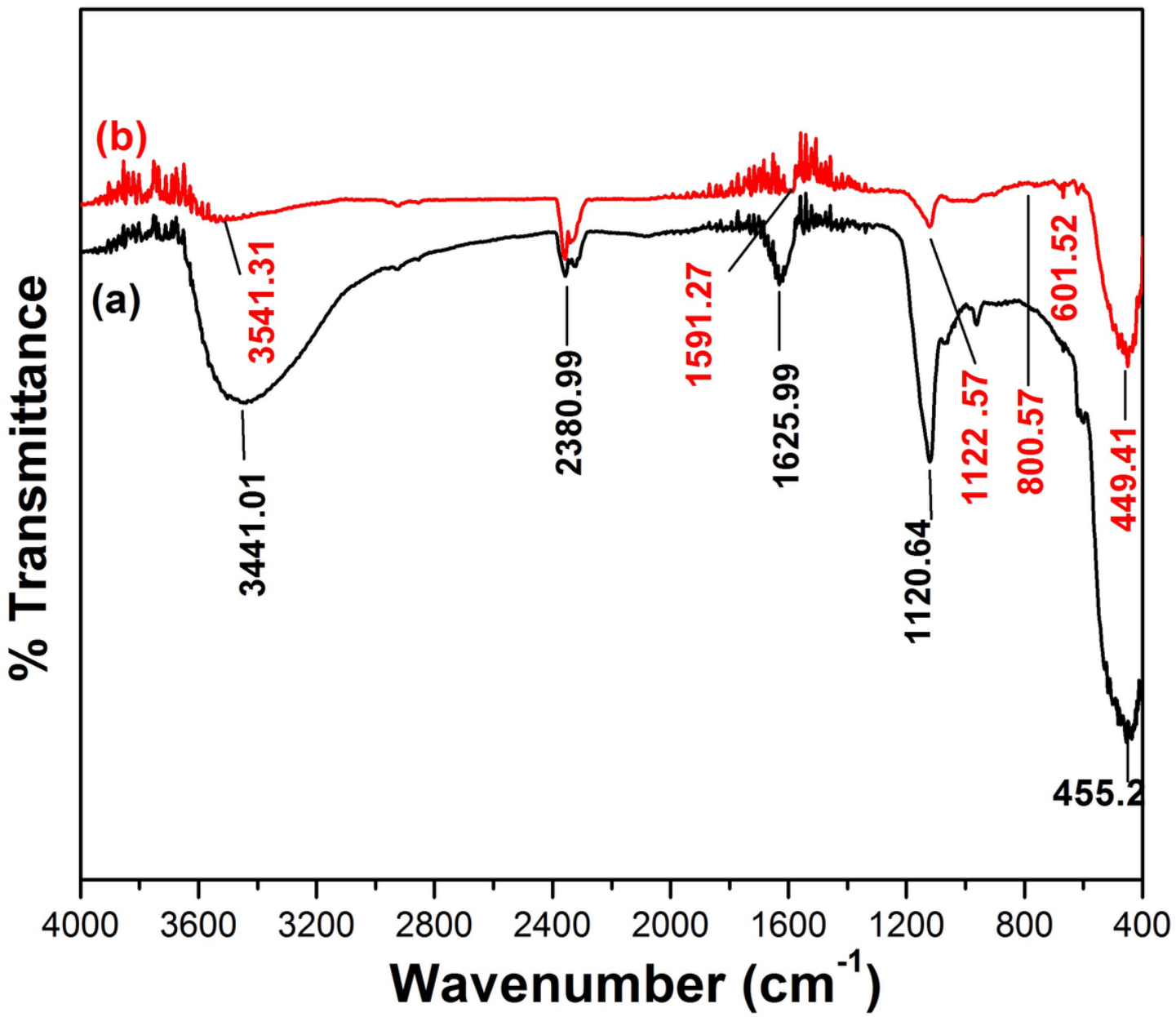

Figure 5

FT-IR spectra of (a) undoped ZnO and (b) 0.1% Fe-ZnO

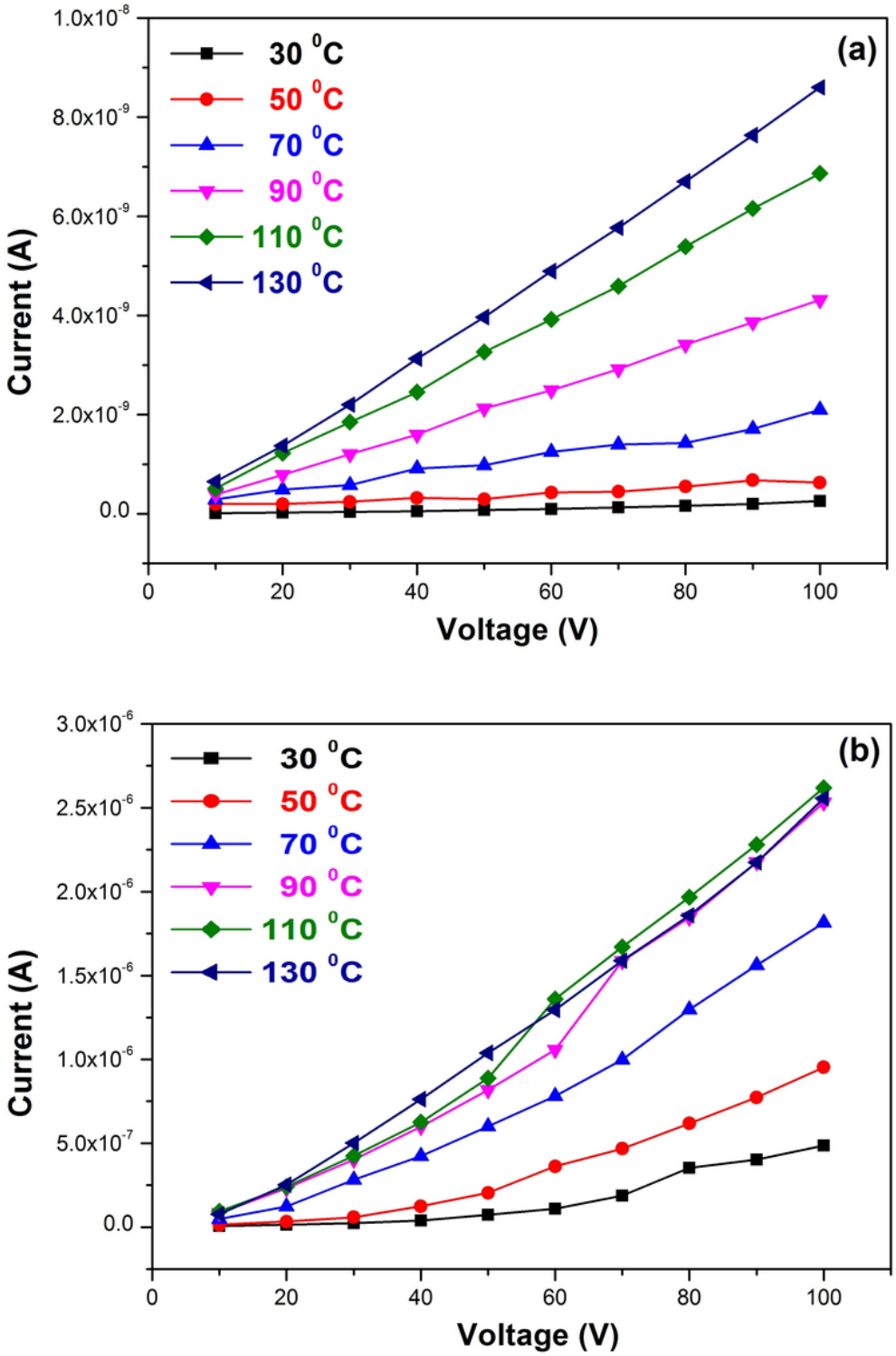

Figure 6

I-V characteristics of (a) undoped ZnO and (b) 0.1% Fe-ZnO.

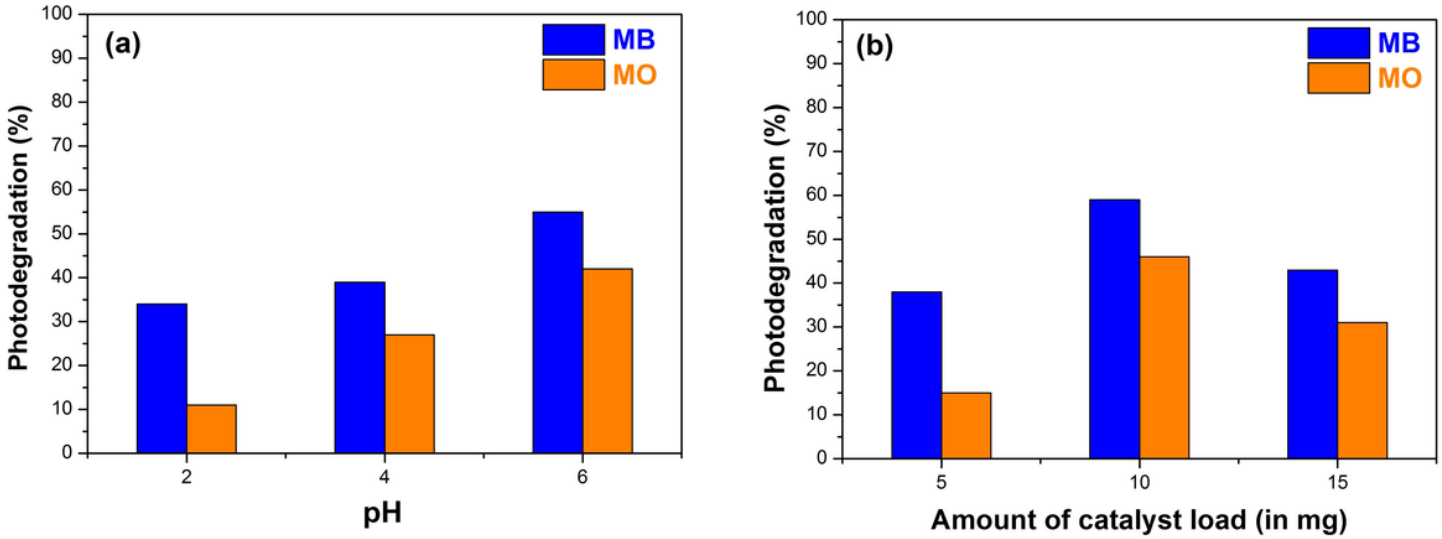

Figure 7

(a) Effect of pH and (b) catalyst concentration on the photodegradation of MB and MO.

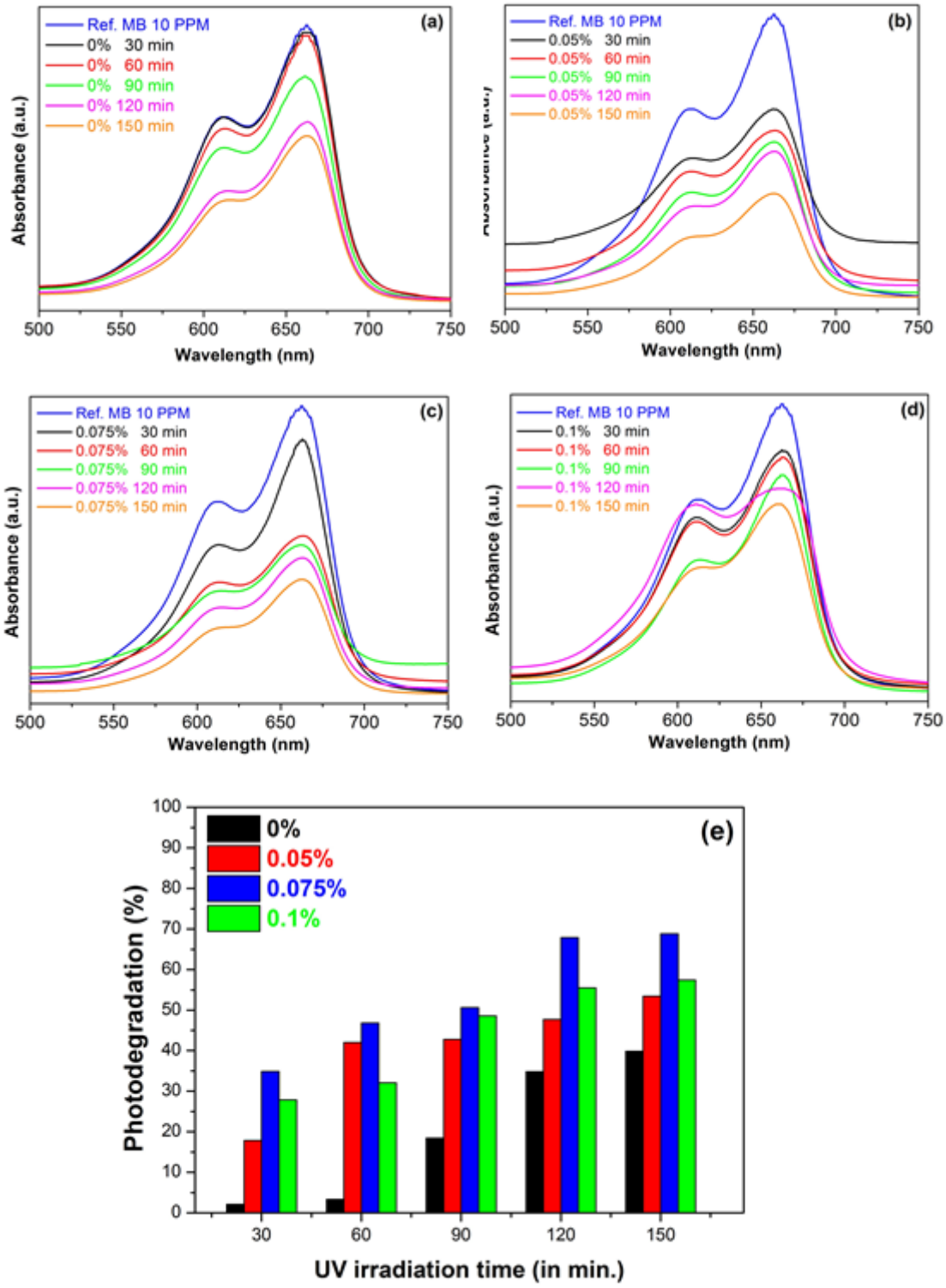

Figure 8

The time dependent UV–Vis absorption spectra of FexZn1-xO nanoparticles with MB dye degradation of (a) undoped ZnO (b) 0.05%, (c) 0.075%, (d) 0.1% and (e) effect of irradiation time on the photodegradation of MB.

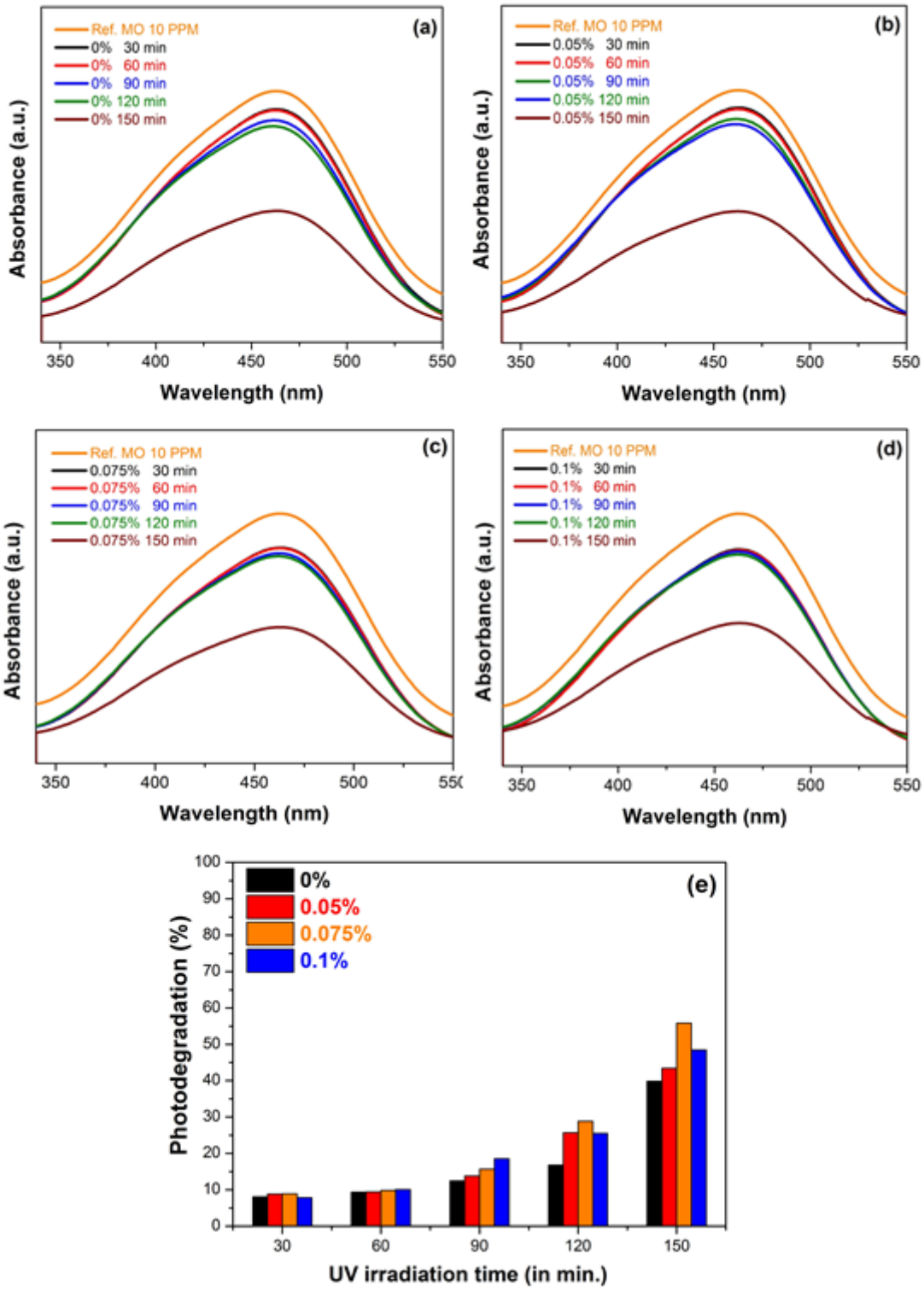

Figure 9

The time dependent UV–Vis absorption spectra of FexZn1-xO nanoparticles with MO dye degradation of (a) undoped ZnO (b) 0.05%, (c) 0.075%, (d) 0.1% and (e) effect of irradiation time on the photodegradation of MO.